

## **In-Service Nondestructive Measurements of Stress-Strain Curves and Fracture Toughness of Oil and Gas Pipelines: Examples of Fitness-for-Purpose Applications**

***Fahmy M. Haggag***

Advanced Technology Corporation

1066 Commerce Park Drive

Oak Ridge, Tennessee 37830, USA

Tel: (865) 483-5756, E-Mail: [Fahmy.Haggag@atc-ssm.com](mailto:Fahmy.Haggag@atc-ssm.com)

Website: [www.atc-ssm.com](http://www.atc-ssm.com)

### **ABSTRACT**

The international transportation networks of oil and gas pipelines are becoming older and beginning to reach their design-lives. This situation brings concerns over pipeline rehabilitation as well as in meeting the current and future energy demands through increasing the transmission throughput safely. This paper describes applications of an innovative Stress-Strain Microprobe (SSM) system that utilizes an *in-situ* nondestructive Automated ball Indentation (ABI) test technique to measure the stress-strain curves and fracture toughness of steel pipelines. The ABI tests provide the actual/current values of these key mechanical properties for base metal, welds, and heat-affected-zones. The SSM-measured key mechanical properties are used with other nondestructive measurements such as crack sizes (determined from smart-pig runs or from other on-line ultrasound devices) to determine the safe operating pressure of the pipeline or to necessitate certain actions of rehabilitation. Examples of SSM test results and their applications in fitness-for-purpose evaluations in the USA, Europe, and Asia, based on deterministic fracture mechanics analysis, are presented in this paper.

### **INTRODUCTION**

Thousands of miles of gas and oil transmission pipelines currently in operation in the USA and other countries have no documentation of their mechanical properties. Section 49 of the US Code of Federal Regulations (CFR) part 192.107 (b) (2) stipulates that for the pipe which is not tensile tested, a yield strength of 165 MPa (24,000 psi) must be used in the equation that determines the design pressure of the pipe section. The Automated Ball Indentation (ABI) test is an *in-situ* nondestructive technique which measures several key mechanical properties of metallic materials. Furthermore, ABI tests provide the actual yield strength values of base metal, welds, and heat-affected-zones which, most of the time, are higher than the conservative CFR value of 165 MPa; thus natural gas or oil up-rating (increasing transmission throughput) can be accomplished safely. Hence, ABI testing of pipelines is a better alternative to the destructive and expensive mechanical tests as demonstrated by this work. This paper summarizes the flow (stress-strain) properties measured by the innovative ABI test technique on many pipeline materials. Moreover, when cracks and other pipeline flaws are produced due to service conditions (e.g. corrosion and/or mechanical damage), the ABI-measured

fracture toughness values can be used in the deterministic structural integrity assessment of the pipeline based on fracture mechanics analysis. Examples of using ABI test results in fitness-for-service analysis are presented in this work.

The laboratory version of the patented [1] Stress-Strain Microprobe (SSM) system has been in commercial use since 1991 in three continents, and the portable SSM version received a 1996 R&D 100 Award (considered by many researchers as the Nobel Prize of Applied Technology). Furthermore, in 1999 Advanced Technology Corporation (ATC) introduced a new miniature SSM system to provide even greater portability and easier field applicability. Equipped with a small, portable battery pack and manual magnetic mounts, this system was proven to be a valuable test instrument for the pipeline industry. The accuracy, reliability, and easy field applicability of the SSM system to test pipeline materials with unknown properties have been demonstrated in this work on samples and on pipeline sections of several major natural gas operators.

The SSM system utilizes an Automated Ball Indentation (ABI) test technique that is described in detail in publications [1-11]. The ABI technique is nondestructive and localized, and is a sophisticated mechanical test technique which can be applied to small samples as well as to metallic components (such as natural gas and oil pipelines) in the field. These capabilities of the ABI technique and the SSM technology are advantageous and desirable for testing aged components and for structural integrity evaluation. One example of such applications is the problem caused by the lack of documentation on some natural gas and oil pipelines. Section 49 of the US Code of Federal Regulations (CFR) part 192.107 (b) (2) stipulates that for the pipe which is not tensile tested, a yield strength of 165 MPa (24,000 psi) must be used in the equation that determines the design pressure of the pipe section. Application of the SSM system to test these pipes will allow the determination of their safe operating pressure, and in many cases can allow up-rating (increasing the transmission pressure) for those pipelines when their SSM-measured yield strength is higher than the low/conservative value of 165 MPa (24 ksi). Furthermore, in addition to the ABI stress-strain curve measurements, the nondestructive and localized ABI technique of the SSM system can provide fracture toughness properties that cannot be obtained from the destructive (and costly for operating pipelines) tensile test. The determination of fracture properties from ABI tests are described elsewhere [7-9] but will be briefly summarized in this paper.

The ABI test is based on progressive indentation with intermediate partial unloadings until the desired maximum depth (maximum strain) is reached and then the indenter is fully unloaded. The indentation load-depth data are collected continuously during the test using a 16-bit data acquisition system. The nonlinear spherical geometry of the tungsten carbide indenter allows increasing strain as the indentation penetration depth is increased. Hence, the incremental values of load and plastic depth (associated with each partial unloading cycle) are converted to incremental values of true-stress and true-plastic-strain according to elasticity and plasticity theories [2,3]. The ABI test is fully automated (using a notebook computer, data acquisition system, and a servo motor) and a single test is completed in less than two minutes depending on the desired strain rate.

As part of this work, miniature tensile tests were fabricated from the pipeline materials with their axes in the circumferential direction. The ABI tests were conducted on the un-deformed end tabs of the miniature tensile specimens using the SSM system. Comparisons of the yield strength values and the stress-strain curves from the ABI and the miniature tensile tests show excellent agreement. Furthermore, a field demonstration of ABI testing was conducted on a 152-mm (6-inch) diameter section of a steel pipe using the new miniature SSM system where the testing head was temporarily mounted to the pipe using two manual magnets having on/off switches. The yield strength and the stress-strain curves from the ABI tests on the pipe are in excellent agreement with those from miniature and large tensile tests of specimens manufactured from the steel pipe. Another successful demonstration of the SSM system was made on a 610-mm (24-inch) diameter X52 steel pipe.

Field testing was also successful on a 914-mm (36-inch) diameter pipe in a refinery in Europe as well as on a 1168-mm (46-inch) diameter natural gas pipeline in Azerbaijan. This work demonstrates the major advantages of the SSM technology to the petroleum industry, namely, its nondestructive, localized, and *in-situ* capabilities. These features make the use of the SSM system, to nondestructively test pipelines with unknown properties, highly desirable to determine the safe operating pressure for the transmission and distribution of natural gas or oil without the need to cut test coupons (e.g., hot tapping), machine destructive specimens, and

repair the test areas. Since this work was completed, commercial use of the SSM system has produced hundreds of successful ABI tests on gas pipelines in the USA, Europe, and Asia.

## RESULTS

Automated Ball Indentation (ABI) and miniature tensile tests were conducted at room temperature on seven materials obtained from two major natural gas operators, namely, ANR Pipeline Company and Columbia Gas Transmission Corporation. The ABI tests were conducted using 0.51-mm and 0.76-mm (0.020-inch and 0.030-inch) diameter tungsten carbide indenters on the end tabs of the miniature tensile specimens, fabricated with their axes in the circumferential direction. The ABI and miniature tensile tests were conducted using the laboratory bench-top configuration of the SSM system. Also as part of this work, the first field demonstration was conducted using the SSM-M1000 system outdoors where it was operated using a small booster battery pack and the testing head was temporarily attached to a 152-mm (6-inch) diameter pipe with two small manual magnets having on/off switches. A field configuration of the SSM system Model SSM-M1000 is shown in Fig. 1. An example of the indentation load-depth curve (using a 0.51-mm diameter indenter) and a typical comparison of the true-stress versus true-plastic-strain curves from ABI and tensile tests are shown in Fig. 2. Detailed summary tables and figures of ABI and tensile tests for all seven pipeline steel materials (Grade B, X42, X52, X60, X42, X52, and X65) are given in Reference [10] (available for downloading from ATC's website: [www.atc-ssm.com](http://www.atc-ssm.com)).

The design of the miniature tensile test specimen was selected to allow manufacturing of specimens with their axes in the circumferential direction for all small and large diameters of the seven pipeline materials. This design was verified earlier at Oak Ridge National Laboratory (ORNL) where the yield strength and ultimate tensile strength values compared very well with those from large tensile specimens [11]. The ABI tests were conducted at room temperature on the end tabs of the miniature tensile specimens, and the stress-strain curves from both techniques were overlaid for comparison. All ABI tests were conducted using 0.51-mm and 0.76-mm (0.020-inch and 0.030-inch) diameter tungsten carbide indenters at indentation speed of 0.0076 mm/s (0.0003 inch/s). The two indenters produced excellent results. However, the smaller size of 0.51-mm (0.020-inch) diameter is more advantageous for use in the field with small, manual magnetic mounts since the maximum indentation load will be less than 400N (90 pounds).

The true-stress and true-plastic-strain values were calculated from the ABI load-depth data using Equations Number 2 through 9 (Ref. 2) where the constraint value " $\alpha_m$ " was taken as 1.3 and 1.2 for the 0.51-mm and 0.76-mm (0.020-inch and 0.030-inch) diameter indenters, respectively. The yield strength value was calculated according to Equations 10, 11, and 14 of Reference [2]. The values of the yield-strength offset-constant and the yield strength slope (Equation 14 in Ref. 2) were determined as -238.6 MPa and 0.3585 (-34.6 ksi and 0.3585) for the 0.51-mm (0.020-inch) diameter indenter while these values were -284.8 MPa and 0.4273 (-41.3 ksi and 0.4273) for the 0.76-mm (0.030-inch) diameter indenter. The true-stress and true-plastic-strain results (including the yield strength point) were fitted to the power law form of Equation 1 of Ref. [2] in order to determine the strain-hardening exponent (equivalent to uniform ductility) and the strength coefficient.

Comparison of the yield strength from ABI tests, using the 0.51-mm and 0.76-mm (0.020-inch and 0.030-inch) diameter indenters, with those from the miniature tensile specimens is shown in Fig. 3. As shown in this figure, the yield strength from ABI tests (using both indenter sizes) and from tensile tests are in excellent agreement where most of the data fell between the  $\pm 5\%$  dashed lines bounding the perfect agreement line (45-degree solid line). A similar agreement was obtained for the ultimate strength values from ABI tests with those from the miniature tensile specimens. Hence, Figs. 2 and 3 demonstrate the reliability and the accuracy of the ABI test technique for testing pipelines.

### Demonstration of SSM Field Testing of Pipelines

The initial ABI testing of a 152-mm (6-inch) diameter carbon steel pipe with a nominal thickness of 7-mm (0.27 inch) was conducted using three sizes of tungsten carbide indenters: 1.57-mm, 0.76-mm, and 0.51-mm (0.062-inch, 0.030-inch, and 0.020-inch) diameter. The testing head of the SSM system was mounted on the pipe using four aluminum V-blocks [10]. Test results on smoothly machined areas were in very good agreement with those from locally polished areas. All ABI tests were carried out up to a maximum

indentation depth of 30% of the indenter radius. The true-stress/true-plastic-strain curves from all three indenter sizes produced the same stress-strain curves despite the various test volumes sampled for each ABI test.

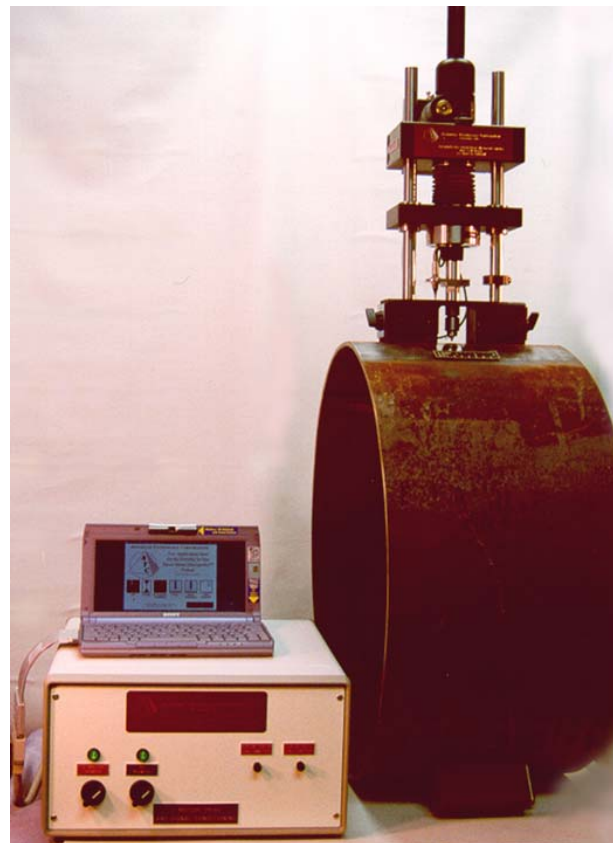


Fig. 1 The testing head of the miniature SSM system is mounted (using manual magnets) on a 610-mm (24-inch) diameter X52 steel pipe section.

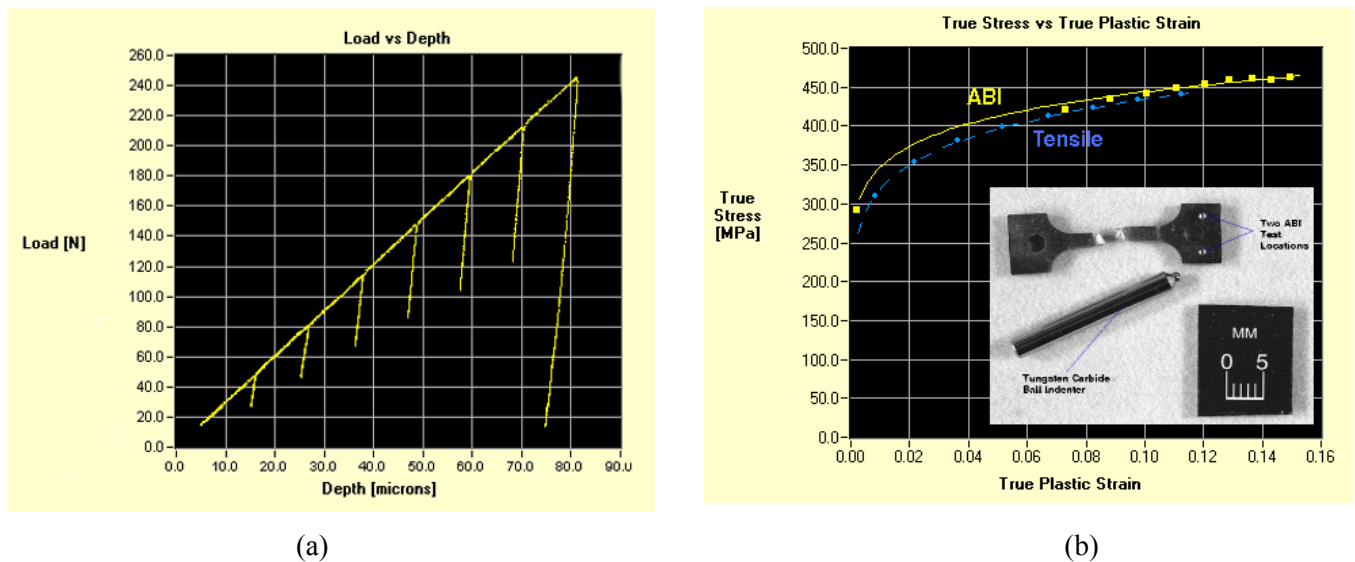


Fig. 2 (a) Indentation load versus depth in an ABI test using a 0.51-mm (0.02-inch) diameter tungsten carbide indenter on X42 ferritic steel material. (b) True-Stress versus True-Plastic-Strain curves from ABI and tensile tests on X42 pipeline steel. A miniature tensile specimen is shown with two indentations made on one end tab with the 1.57-mm diameter tungsten carbide indenter shown in the inset photo.

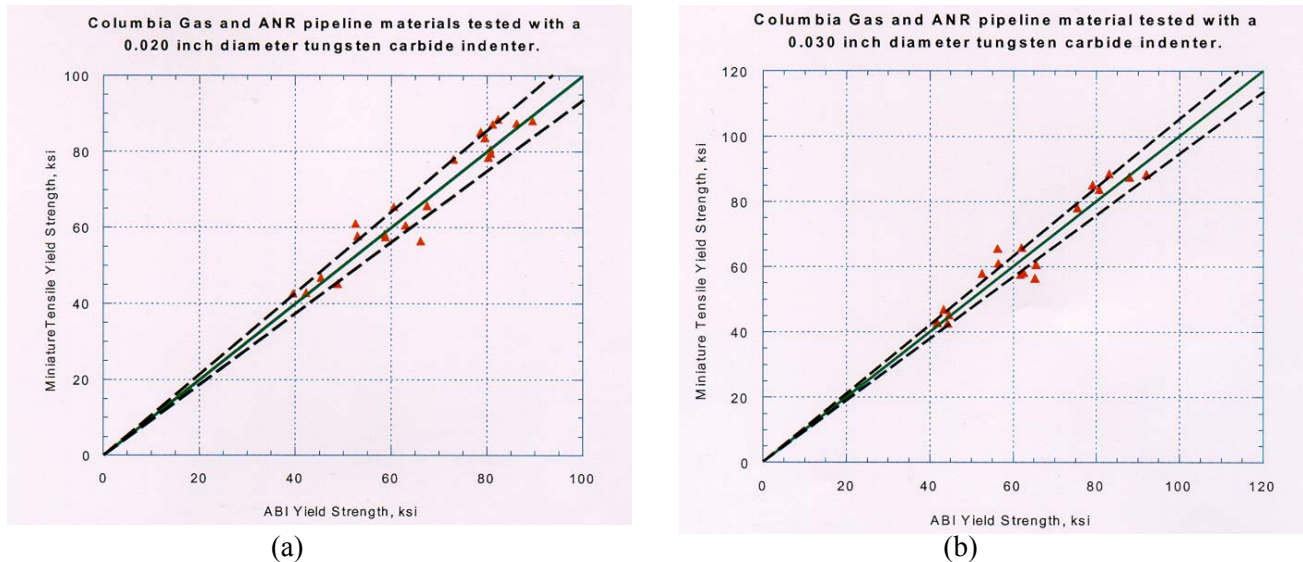


Fig. 3 Comparison between yield strength from ABI tests and miniature tensile tests: (a) using a 0.51-mm diameter indenter, (b) using a 0.76-mm diameter indenter. The dashed lines represent the  $\pm 5\%$  variation from perfect agreement (45-degree solid line). (1 ksi = 6.895 MPa).

A field demonstration was conducted using the miniature Portable/In-Situ Stress-Strain Microprobe system (Model SSM-M1000) outdoors where it was operated using a small booster battery pack and the testing head (weighing 10 kg) was temporarily attached to a 152-mm diameter carbon steel pipe (obtained from Columbia Gas Transmission Corporation) with two small manual magnets having on/off switches. Both the 0.51-mm and 0.76-mm (0.020-inch and 0.030-inch) diameter indenters produced successful ABI test results using the magnetic mounts. The yield strength and stress strain curves from ABI tests on the pipe section and on the end tabs of miniature tensile specimens (fabricated from the pipe section) were in very good agreement with those from the test results of miniature tensile specimens. Another successful SSM field demonstration was conducted on a 610-mm (24-inch) diameter X52 pipeline.

### Determination of Fracture Toughness Master Curve from ABI Tests

Indentation with a small ball indenter generates concentrated stress (and strain) fields near and ahead of the contact of the indenter and the test surface, similar to concentrated stress fields ahead of a crack albeit the indentation stress fields are mostly compressive. The high value of the stress under the ball indenter is sometimes called an example of *plastic constraint* where it is the rigid material surrounding the indentation volume that does the constraining. Hence, at a certain critical ball indentation depth there is a high state of transverse and lateral stresses similar to those in front of a sharp notch in an elastic material. Although, the conditions for crack initiation might be attained, the high degree of plastic constraint is the reason that cracks do not develop during ball indentation of ductile metallic materials. This explains that only initiation fracture toughness and no tearing modulus can be determined from ball indentation. The initiation fracture toughness is calculated from the integration of indentation deformation energy up to the critical depth (when the maximum pressure underneath the ball indenter equals the critical fracture stress of the steel material) as described in detail elsewhere [7, 9]. Examples of the ABI-measured fracture toughness results on plate and weld steel materials are shown in Figs. 4 and 5. The new ABI-measured fracture toughness capability is, in practical terms, material thickness independent (since small indenters can be used for all pipelines and pressure vessels). Furthermore, its localized nature allows testing heat-affected-zones that cannot be tested destructively because of their irregular shape and small volumes.

### How can fracture toughness of ferritic steels be determined from the ABI test ?

It is agreed upon that an ABI test does not produce fracture in a metallic test sample (because of the plastic constraint and the ductility of the test material) and that there is no fatigue crack requirement for the ABI test (which makes it nondestructively attractive). However, the simple reasons (without the use of equations) for

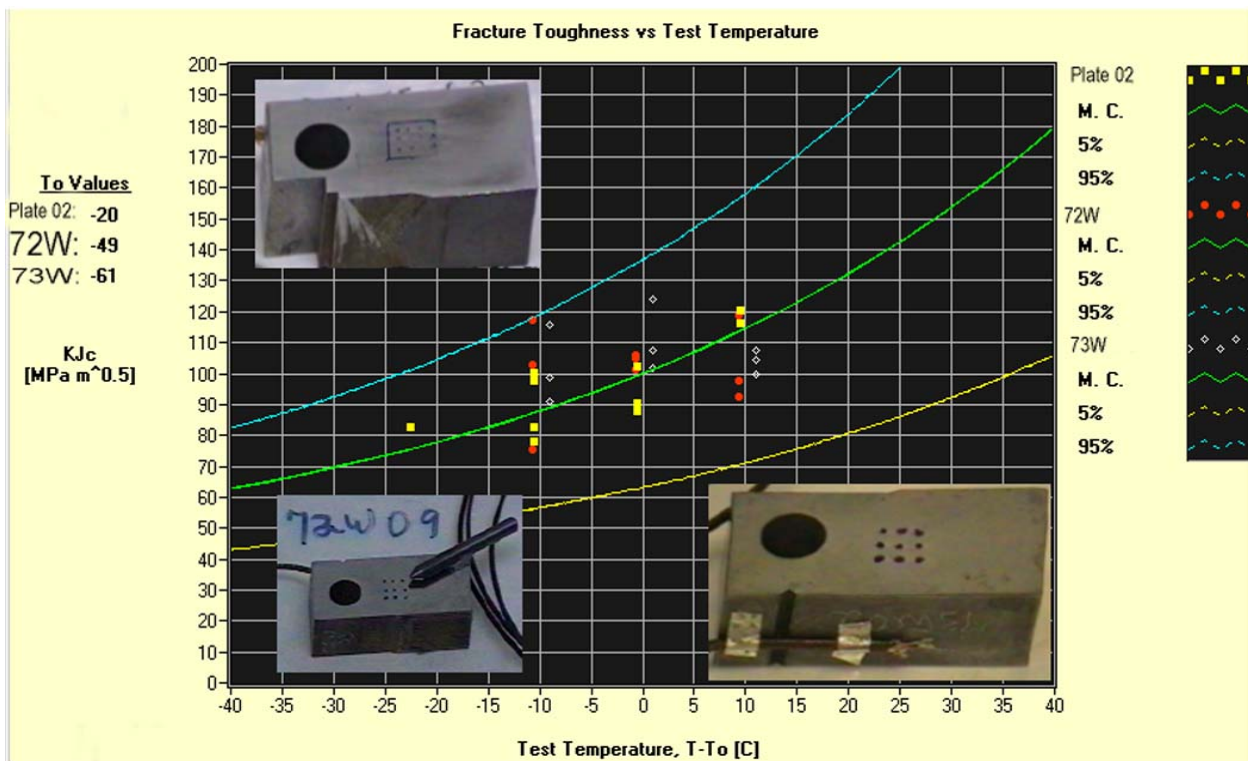


Fig. 4 Fracture toughness Master Curve obtained from ABI tests on three reactor pressure vessel steels. A 0.51-mm (0.020-inch) diameter tungsten carbide indenter was used to perform 11 ABI tests on Plate 02 (the specimen on the top left of the figure), and 9 ABI tests each on the 72W and 73W weld samples (shown on the left and right lower part of the figure, respectively). The ABI-determined reference temperatures of the three materials were within 5°C of the values from the pedigree destructive fracture toughness tests.

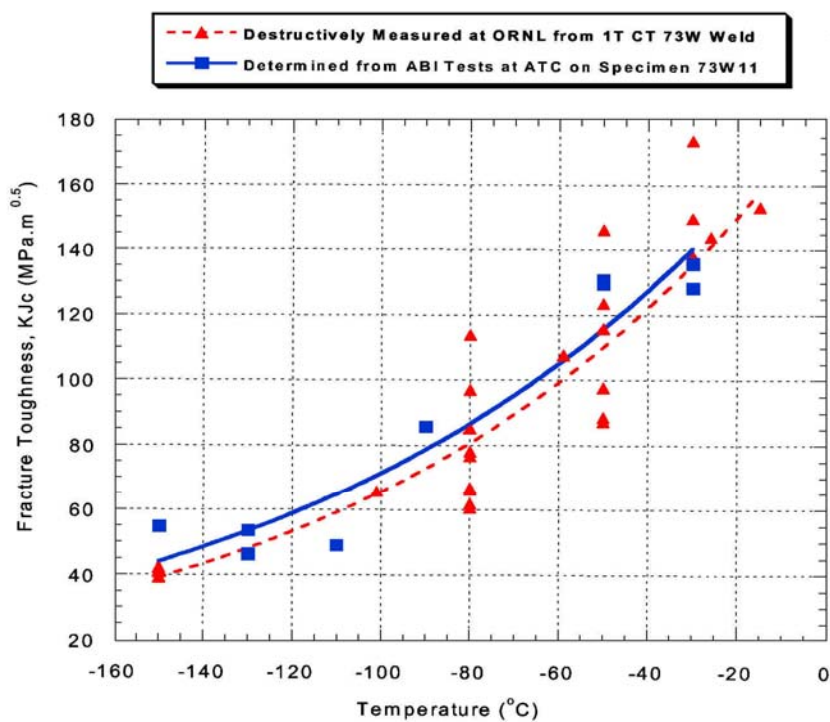


Fig. 5 Comparison between nondestructively ABI-measured ( $K_{Jc}^{ABI}$ ) performed at ATC (using a 1.57-mm indenter) and destructive 1T CT fracture toughness test results of 73W weld of ORNL.

the success of this technique to determine fracture toughness of ferritic steels in the transition region are: (1) the attainment of a high degree of stress-triaxiality (stress concentration similar to that ahead of a crack-tip) because of the plastic constraint provided by the test material surrounding the spherical indentation, (2) the increase of the value of maximum stress (110% of the mean pressure in the material beneath the ball indenter) with increasing indentation depth until reaching or exceeding (at some low test temperatures) the critical fracture stress of the material, and (3) the fracture of ferritic steels at low temperatures in the transition region is controlled by the critical fracture stress of the material.

At a critical indentation depth (when the maximum stress underneath the ball indenter equals the critical fracture stress), the deformation energy (integration of the area under the indentation load versus indentation depth up to the critical indentation depth, in the same units as the J-integral) represents the temperature dependent part of the fracture toughness of the test material. A temperature-independent value of  $30 \text{ MPa}\cdot\text{m}^{0.5}$  is added to the ABI-determined fracture toughness value, similar to the equation of the fracture toughness master curve of ASTM Standard E1921-97. The fact that during an ABI test all the requirements to calculate the initiation fracture toughness are achieved at a critical deformation energy depth allows the determination of fracture toughness without any crack propagation (the latter is prevented by the high plastic constraint of the test material surrounding the spherical indentation). Hence, only fracture toughness initiation and no tearing modulus can be determined from the ABI test.

Researchers at ATC have produced cracks in two perpendicular directions in a sodium chloride single crystal using a 1.5-mm diameter ball indenter (work performed by ATC for the US Navy, see Fig. 6) which is a proof that the maximum stress underneath the ball indenter reached the fracture stress of the single crystal.

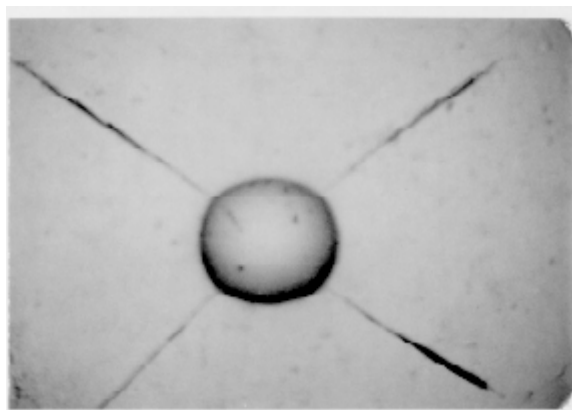


Fig. 6 Cracks produced with a 1.5-mm diameter ball indenter in a sodium chloride single crystal.

Moreover, in the non-standardized bulge test (sometimes called small punch test) a very thin sheet of metal is clamped in a die, and a punch with a large spherical end is pushed against one surface of the thin sheet until the sheet is fractured on the opposite/tensile side. However, fracture toughness cannot be calculated from the plane stress bulge test. In the bulge test, fracture occurs even though the specimen does not contain any fatigue crack prior to the test.

In an ABI test, the maximum stress underneath the indenter increases with depth but fracture does not occur because of the plastic constraint of the material surrounding indentation (the specimen or the structure thickness must be ten times the maximum indentation depth to avoid back surface effects and to obtain valid ABI test results). Furthermore, in a destructive  $J_{Ic}$  fracture toughness test, although we propagate/extend the fatigue crack, we extrapolate the power-law-fit of the J-integral versus crack extension curve to intersect a line parallel to the blunting line (0.2 mm offset line) where the intersection point determines the  $J_{Ic}$  initiation fracture toughness. This procedure is required since it is very difficult to stop loading the sample at the appropriate deformation energy level associated with the onset of crack extension from the pre-existing fatigue crack of the destructive fracture toughness specimen. This means that the fracture toughness value determined from the destructive test is actually the deformation energy up to the point of initial crack extension. Hence, the capability to determine fracture toughness from the ABI test without having to machine

and fatigue crack a specimen is a truly innovative method, and it is the only method for *in-situ* direct measurement.

Furthermore, the current and challenging need for numerous industrial applications is to obtain fracture toughness of ferritic steel structures without cutting boat samples or hot tapping to machine miniature fracture specimens. Miniature specimens produce invalid fracture toughness values most of the time because of the violation of the geometry requirements for plane strain. For example, many pipelines and vessels are not manufactured in the large thickness required to obtain valid fracture toughness test results, and often the owner of such components will not allow hot tapping or the cutting of a boat sample regardless of its size. Moreover, ABI tests will produce valid fracture toughness values all the time while the current ASTM destructive methods may never produce valid test results. Another great advantage of the ABI test method is its applicability to small welds and heat-affected-zones where the current ASTM standard test techniques might not be feasible.

Moreover, recent developments at ATC allow ABI testing at ambient temperature and determining the fracture toughness at other temperatures of interest (using the fracture toughness master curve concept and the appropriate critical fracture stress or strain model depending on the actual test temperature). Furthermore, dynamic fracture toughness values could be estimated from the measured static fracture toughness and yield strength test results.

### **Determination of the Indentation Energy to Fracture (*IEF*)**

A new ABI energy parameter called *Indentation Energy to Fracture (IEF)* was developed for ferritic steels [7]. This *IEF* parameter allows the nondestructive determination of fracture energy from the ABI-measured mean indentation pressure up to a critical indentation depth (according to the controlling micro-mechanical fracture mechanism of the critical fracture stress or the critical fracture strain, depending on the test temperature). The indentation load versus depth curves from ABI tests at various temperatures were used together with the critical fracture stress model to determine the fracture toughness from the indentation deformation energy. The development of the *IEF* parameter is based on the following:

- (a) Fracture toughness can be interpreted as the deformation capability of the material under a concentrated stress field.
- (b) Indentation with a small ball indenter generates concentrated stress (and strain) fields near and ahead of the contact of the indenter and the test surface, similar to concentrated stress fields ahead of a crack albeit the indentation stress fields are mostly compressive. The high value of the stress under the ball indenter is sometimes called an example of *plastic constraint* where the rigid material surrounding the indentation volume that does the constraining. Hence, at a certain critical ball indentation depth there is a high state of transverse and lateral stresses similar to those in front of a sharp notch in an elastic material. Although, the conditions for crack initiation might be attained, the high degree of plastic constraint is the reason that cracks do not develop during ball indentation of ductile metallic materials. This explains that only initiation fracture toughness and no tearing modulus can be determined from ball indentation.
- (c) Monotonic tensile and compressive stress-strain curves are similar which is true for most homogenous metallic structural materials.
- (d) The cleavage fracture stress in ferritic steels is nearly temperature insensitive at very low test-temperatures in the transition and low shelf regions.
- (e) The deformation energy due to ball indentation up to a limit mean pressure level is related to the fracture toughness; the limit stress, attained at a critical indentation depth in an ABI test, is proportional to the critical fracture stress of the test material.

The *IEF* is thus defined as:

$$IEF = \int_0^{h_f} P_m(h) dh \quad (1)$$

where,

$$P_m = \frac{4P}{\pi d^2} \quad (2)$$

In the above equation,  $P_m$  is the mean indentation contact pressure,  $P$  is the indentation load,  $h$  is the indentation depth,  $h_f$  is the indentation depth when the value of the mean pressure multiplied by 1.1 is equal to the critical fracture stress (i.e,  $P_m \times 1.1 = \text{fracture stress}$ ), and  $d$  is the chordal diameter of the indentation. It is important to note that the mean pressure under a spherical indentation increases with increasing indentation depth and with decreasing test temperature in ferritic steels.

$$d = 2(Dh - h^2)^{0.5} \quad (3)$$

### Determination of fracture toughness ( $K_{Jc}$ )<sup>ABI</sup> from ABI tests at various temperatures

The Charpy impact energy and the static fracture toughness,  $K_{Jc}$ , have non-zero lower shelves even at very low test temperatures. Hence, the fracture energy per unit area,  $W_f$ , can be given by:

$$W_f = W_o + W_T \quad (4)$$

where  $W_o$  is the lower shelf energy per unit area, and  $W_T$  is the temperature-dependent energy to be calculated from Equation 1 (i.e. ,  $W_T = IEF$ ).

For ferritic steels (with yield strength of 275 to 825 MPa or 40-120 ksi) the fracture toughness (median value) versus temperature curve in the transition temperature region is expressed by the master curve (ASTM E-1921-97):

$$K_{Jc}(\text{med}) = 30 + 70e^{0.019(T-T_0)} \quad \text{MPa}\sqrt{\text{m}} \quad (5)$$

where  $T$  is the test temperature and  $T_0$  is the reference temperature when  $K_{Jc} = 100 \text{ MPa}\sqrt{\text{m}}$ . From the above equation, the lower shelf fracture toughness,  $W_o$ , is  $30 \text{ MPa}\sqrt{\text{m}}$ . The fracture toughness determined from ABI tests can then be calculated from:

$$(K_{Jc})^{ABI} = 30 + \sqrt{2E(W_T)} \quad (6)$$

where  $E$  is the elastic modulus.

### Example of the Use of ABI tests in a Fitness-for-Service Assessment

A catastrophic failure occurred in a natural gas plant in a cold winter night shortly following the leak of a liquid natural gas into the line. The combination of cold temperature and high strain rate near a crack resulted in the destruction of approximately 12-meter section of a 508-mm (20-inch) diameter pipeline into several hundred small pieces. The plant operator was concerned that the pipeline steel might not have the appropriate flow and fracture properties since the fracture surfaces of many small pieces indicated brittle fracture. Although, the pipeline piece containing the crack was not found at the time of ATC's report, the ABI tests on several small pieces confirmed that the pipeline steel material meet the mechanical properties specified for the seamless carbon steel pipe at the time of construction. Multiple ABI tests were conducted, on a block machined from a small steel piece, at several low temperatures using ATC's patented Portable/In-Situ Stress-Strain Microprobe<sup>TM</sup> (SSM) system. All ABI tests were conducted using a 0.51-mm (0.020-inch) diameter tungsten carbide indenter at a speed of 0.01-mm/s (0.0004 in/s), or a strain rate of 0.014/s, to a maximum indentation depth of 0.076-mm (0.003-inch). Stress-strain curves and fracture toughness values were measured from the individual ABI tests. In addition, the fracture toughness median curve as well as its 95% and 5% confidence limit curves were determined from the ABI tests. The reference temperature,  $T_o$ , defined in the ASTM Standard E1921-97 [Ref. 12, "Standard Test Method for Determination of Reference Temperature,  $T_o$ , for Ferritic Steels in the Transition Range,"] as the test temperature corresponding to a median fracture toughness level of  $100 \text{ MPa}\sqrt{\text{m}}$  ( $90.9 \text{ ksi}\sqrt{\text{in}}$ ), was determined from the ABI tests at several low test temperatures. The ABI tests determined a  $T_o$  value of  $-24^\circ\text{C}$  for the base metal of the pipe.

The ABI-determined  $T_0$  value demonstrates that the pipeline material has good static fracture toughness of  $100 \text{ MPa}\sqrt{\text{m}}$  at a low temperature of  $-24^\circ\text{C}$  that is lower than normal pipeline operating temperature in winter. However, these ABI-measured good static fracture toughness values do not prevent brittle failure that might result from the existence of any small crack (developed during pipeline service) and due to the combination of very low temperature and a dynamic loading at a high strain rate (it should be noted that all carbon steels have a lower/brittle fracture toughness shelf with a median value of  $30 \text{ MPa}\sqrt{\text{m}}$  regardless of their various values of much higher fracture toughness at higher operating temperatures).

The fracture toughness values were calculated from ABI tests according to the procedures described in Reference 7. Examples of the graphical and printed test data and results from a single ABI test [ML-28-4 conducted at  $-33^\circ\text{C}$  ( $-28^\circ\text{F}$ )] are shown in Figures 7-11. Fig. 7 shows the ABI indentation load versus depth data using a single-cycle ABI test technique (without any intermediate partial unloading). The yield strength calculation plot is shown in Fig. 8 where “P” is the load, “dt” is the chordal diameter of indentation at various depth values, and “D” is the indenter diameter. Figure 9 shows the true-stress/true-plastic-strain curve where the yield strength value (plotted as a solid symbol) was calculated from Fig. 8 as described in Reference 2. Fig. 10 shows the maximum pressure (calculated as 110% of the mean pressure underneath the indenter as discussed in Reference 7) as a function of normalized indentation depth (dt/D). It is important to note that the maximum pressure increases with increasing indentation depth. When the value of the maximum stress equals the critical fracture stress (340 ksi) the critical of “dt/D” is used to calculate the critical indentation depth for integrating the area under the indentation load/depth curve to calculate the J-integral and the fracture toughness of the test sample. In this ABI example, the critical “dt/D” and the critical indentation depth are 0.31 and 12.45 microns as shown on the printed test results shown in Fig. 11. The ABI-determined fracture toughness reference temperature ( $T_0$ ) value is  $-24^\circ\text{C}$ . The fracture toughness median curve and its 95% and 5% confidence limit curves are shown in Figure 12.

In Figure 10, note that the maximum stress at this low test-temperature of  $-33^\circ\text{C}$  ( $-28^\circ\text{F}$ ) increases well beyond the critical fracture stress up to a value of  $2760 \text{ MPa}$  (400 ksi) at a dt/D value of 0.75 (the later represents the end of the ABI test at a depth of 12.45 microns). The high values of the maximum stress were attainable because of the multi-axial nature of the ABI test that provides a high degree of stress-triaxiality (stress concentration) underneath the spherical indenter due to the high degree of plastic constraint provided by the ductile material surrounding the indentation. This is in contrast to the uniaxial tensile test that does not provide enough constraint in the specimen gage section, and its maximum stress is attained at the ultimate tensile strength (specimen necking). The ultimate strength for many structural steels is less than  $830 \text{ MPa}$  (120 ksi) that is much lower than the critical fracture stress of the material. Figure 9 illustrates that although the ABI test provides tensile properties, it also measures fracture toughness because of its triaxial stress loading nature. Several text books describe the area under a tensile stress-strain curve as an estimate of fracture toughness which is incorrect since the tensile test does not provide the required constraint and its units are in  $\text{MPa}$  (ksi) and not in the appropriate fracture toughness units of  $\text{MPa}\sqrt{\text{m}}$  ( $\text{ksi}\sqrt{\text{in}}$ ).

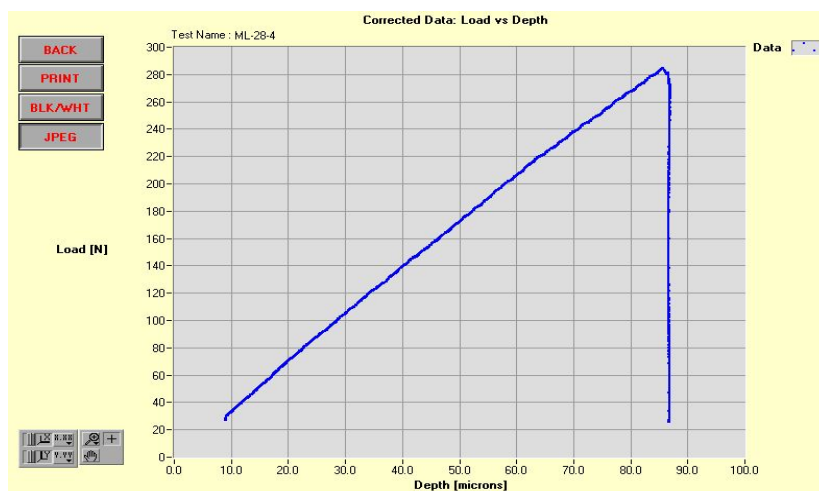


Fig. 7 Indentation load versus depth using the single-cycle ABI test technique.

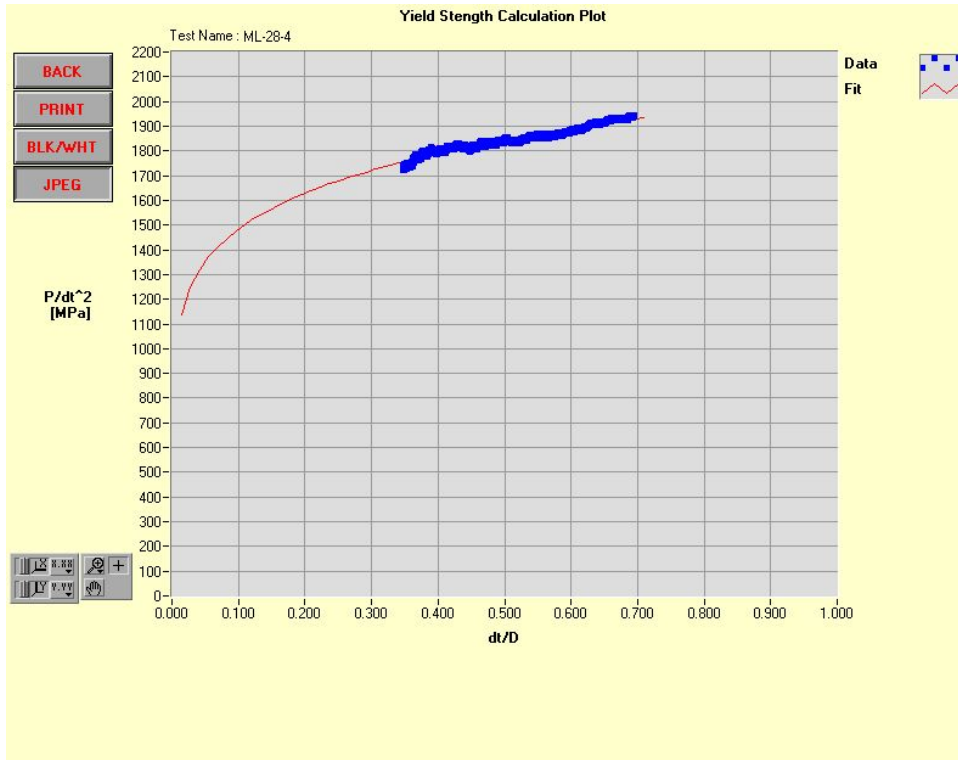


Fig. 8 Yield strength calculation plot.

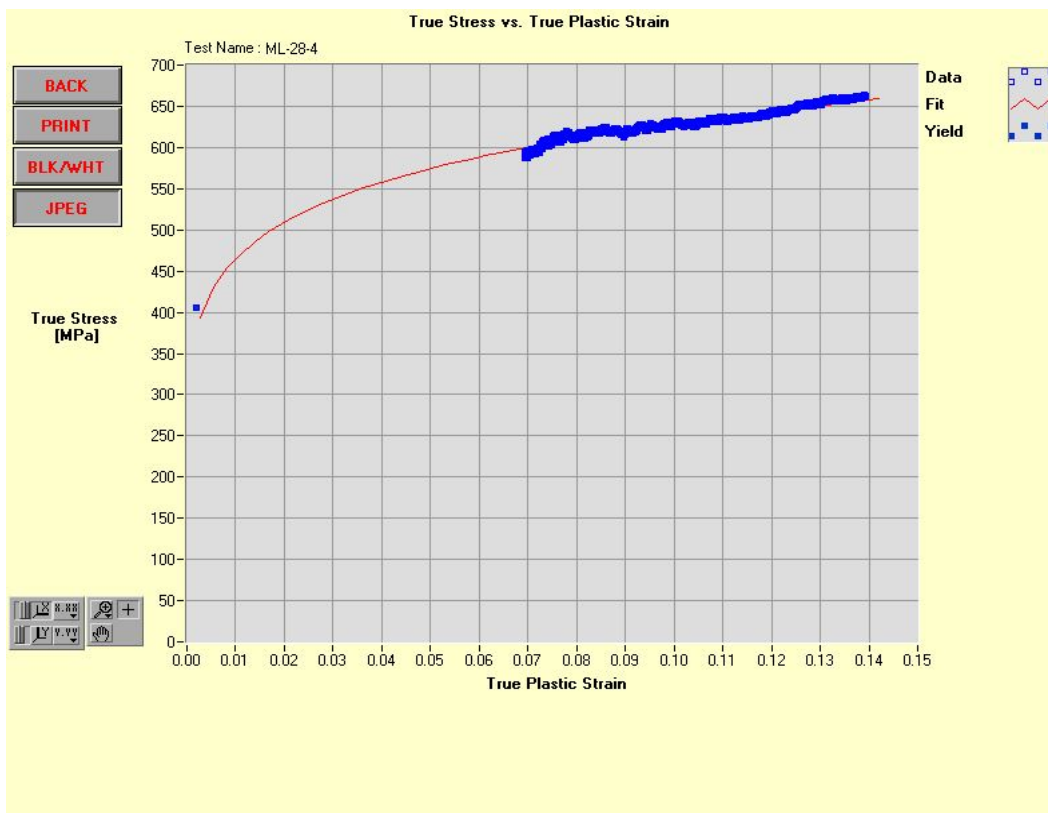


Fig. 9 True-stress/True-strain plot.



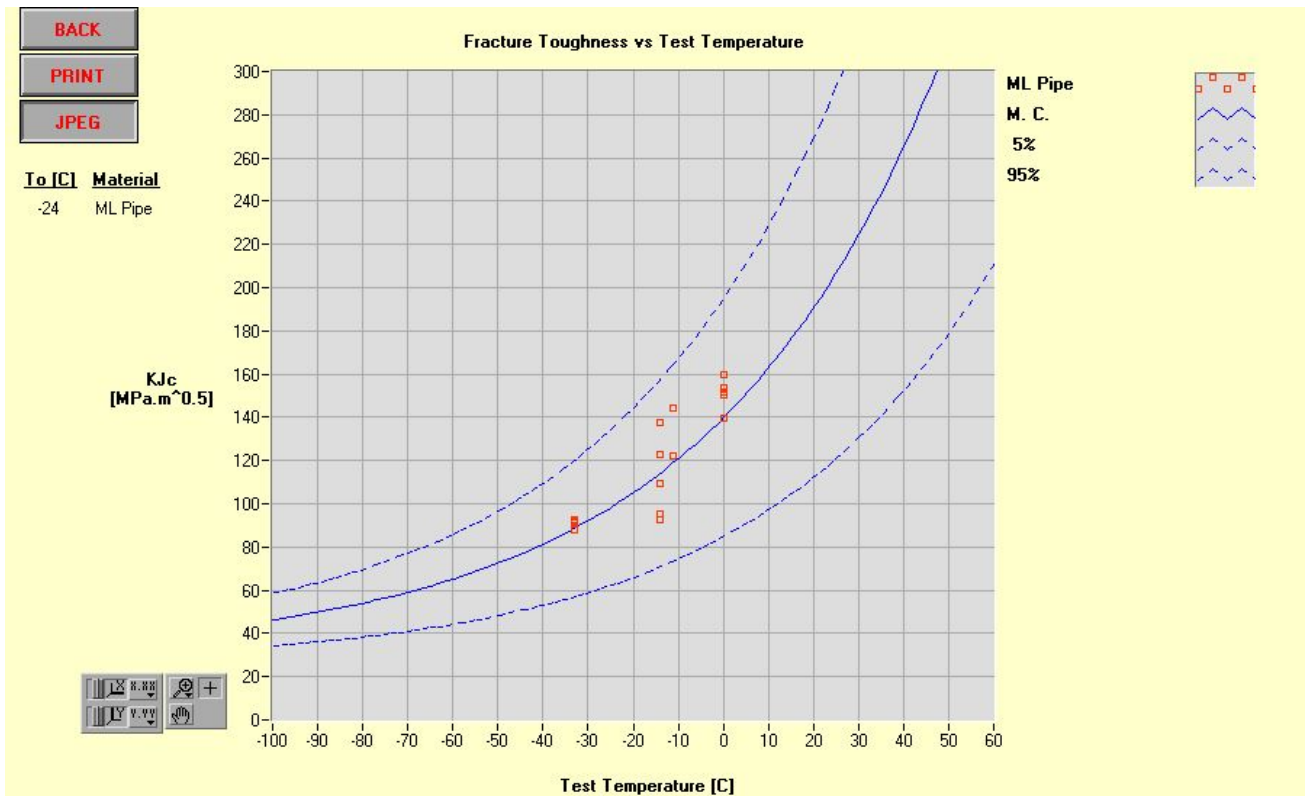


Fig. 12 Static fracture toughness  $K_{Jc}$  determined from 17 ABI tests conducted on pipeline steel sample at four test temperatures.

Triplicate ABI tests were conducted at room temperature on the same pipe steel sample, and the fracture toughness values were calculated from the indentation load-depth data using the critical fracture strain model instead of using the critical fracture stress model that was used earlier for analyzing ABI tests at low test temperatures. The critical-strain (empirically determined) for this new analysis was 0.14 (14%). This new method produced slightly conservative fracture toughness values and the reference temperature value determined from the room temperature ABI tests was  $-19^{\circ}\text{C}$  (slightly higher than the  $-24^{\circ}\text{C}$  value determined from low-temperature ABI tests). It should be noted that the ABI tests at room temperature [ $22^{\circ}\text{C}$  ( $72^{\circ}\text{F}$ )] did meet the ASTM requirement for applying the Weibull statistical master curve fitting since they were within the  $\pm 50^{\circ}\text{C}$  of the reference temperature for this pipeline material. The new critical fracture strain method analyzing the ABI test data at room temperature was also applied to three pressure-vessel steel materials (Plate 02, and Welds 72W and 73W shown earlier in Fig. 4), and the reference temperatures were also conservative as compared to those from destructive fracture toughness and from ABI tests at low test temperatures.

In order to obtain median dynamic fracture toughness ( $K_{Id}$ ) values as a function of temperature, the ASTM Standard E1921-97 equation of the static fracture toughness ( $K_{Jc}$ ) master curve (Reference 12) can be used provided that the reference temperature be shifted to a higher value by the amount of  $78^{\circ}\text{C}$  ( $140^{\circ}\text{F}$ ). It is well known that the dynamic fracture toughness curve is shifted to the right hand-side of the static fracture toughness curve by a temperature shift value depending on the room-temperature yield strength of the ferritic steel material.

The median dynamic fracture toughness ( $K_{Id}$ ) can be calculated from the following equation:

$$K_{Id}(med) = 30 + 70e^{0.019(T-[T_0+T_{shift}])} \quad \text{MPa}\sqrt{\text{m}} \quad (7)$$

Where  $T$  is the test temperature in  $^{\circ}\text{C}$  and  $T_0$  is the reference temperature when  $K_{Jc} = 100 \text{ MPa}\sqrt{\text{m}}$ . The  $T_0$  value, determined from the ABI tests at low test-temperatures, to be used in the above equation is  $-24^{\circ}\text{C}$ . The  $T_{shift}$  of  $78^{\circ}\text{C}$  ( $140^{\circ}\text{F}$ ) was determined from the Barsom correlation [Ref. 13] and using the average yield strength of 50 ksi that was measured from multiple ABI tests at room temperature. The Barsom correlation is given by:

$$T_{shift} (^{\circ} F) = 215 - 1.5\sigma_{ys} (ksi) \quad \text{for } 36 \text{ ksi} < \sigma_{ys} < 140 \text{ ksi} \quad (8)$$

where  $\sigma_{ys}$  is the room-temperature yield strength of the steel material.

The static and dynamic fracture toughness median curves for the pipeline steel are provided in Figure 13.

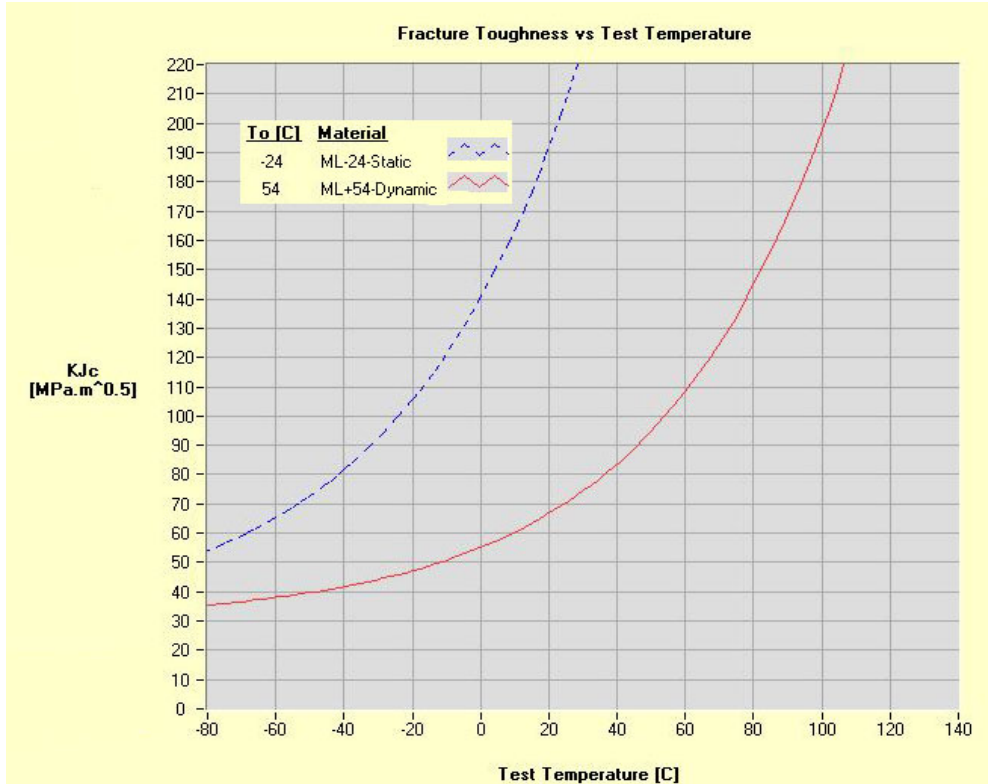


Fig. 13 The dynamic median fracture toughness curve is calculated from the ABI-determined static fracture toughness master curve of the pipeline steel sample by shifting the static curve to the right by 78°C.

## SUMMARY AND CONCLUSIONS

The results presented briefly in this paper and in detail in Refs. [7,10] demonstrate the capabilities of ATC's patented Portable/In-Situ Stress-Strain Microprobe (SSM) system and its Automated Ball Indentation (ABI) test technique to nondestructively measure the yield strength, the stress-strain curve, and fracture toughness of carbon steel materials, from various natural gas pipeline manufacturers, in a reliable and accurate manner on samples and components.

The accuracy, reliability, and easy field applicability of the SSM technology to test pipeline materials with unknown properties have been demonstrated in this work. Reference [10] was reviewed favorably by the US Office of Pipeline Safety (OPS) in December 1999 and the SSM technology is recommended for use by the pipeline industry. The test results of Reference [10] work provide the technical basis for: (1) a pipeline operator to submit a waiver to the OPS of the US Department of Transportation (DOT) to use the ABI test as an alternative to the tensile test, and (2) preparing an Amendment to 49 CFR 192 Appendix B to allow nondestructive ABI testing as an alternative to the destructive and expensive tensile testing to measure the yield strength and the stress-strain curve of steel pipeline with unknown properties. The laboratory version of the SSM system has been in commercial use since 1991 in three continents, and the portable SSM version received a 1996 R&D 100 Award. Furthermore, the miniature SSM-M1000 was introduced by ATC in 1999 to provide even greater portability. Equipped with a portable battery pack and manual magnetic mounts, the SSM-M1000 proved to be a valuable test instrument for the pipeline industry. The use of the SSM system to

test pipelines in the field will improve their structural integrity evaluation as well as their operational efficiency (by allowing safe up-rating).

## ACKNOWLEDGMENTS

Advanced Technology Corporation (ATC) would like to thank ANR Pipeline Company and Columbia Gas Transmission Corporation for providing several steel pipeline materials (various grades manufactured from 1931 through 1978) to perform the destructive tensile and the nondestructive Automated Ball Indentation (ABI) tests at ATC. The tensile and ABI tests were conducted using ATC's patented Portable/In-Situ Stress-Strain Microprobe (SSM). We extend our sincere thanks to Mr. Ted Clark (Columbia Gas), Mr. Richard Eckert (ANR Pipeline), and Dr. Jude Foulds (Exponent) for attending the miniature tensile testing, ABI blind testing, and the demonstration of the SSM system to test a full-cylindrical pipe section at ATC on June 22 and 23, 1999. The continued encouragement of Mr. Gopala Vinjamuri (Office of Pipeline Safety, US DOT) and Dr. John H. Smith (retired from the Metallurgy Division, National Institute of Standards and Technology, Gaithersburg, MD) during this work is greatly appreciated. Major funding of the ABI-measured fracture toughness development was provided by the US Department of Energy.

## REFERENCES

- [1] Haggag, F. M., "Field Indentation Microprobe for Structural Integrity Evaluation," U.S. Patent No. 4,852,397, 1989.
- [2] Haggag, F. M., "In-Situ Measurements of Mechanical Properties Using Novel Automated Ball Indentation System," *ASTM STP 1204*, 1993, pp. 27-44.
- [3] Haggag, F. M., et al., "Use of Portable/In Situ Stress-Strain Microprobe System to Measure Stress-Strain Behavior and Damage in Metallic Materials and Structures," *ASTM STP 1318*, 1997, pp. 85-98.
- [4] Haggag, F. M. et al., "Structural Integrity Evaluation Based on an Innovative Field Indentation Microprobe," *ASME PVP-Vol. 170*, 1989, pp. 101-107.
- [5] Druce, S. G., et al., "The Use of Miniature Specimen Techniques for the Assessment of Material Condition," *ASME PVP-Vol. 252*, 1993, pp. 58-59.
- [6] Byun, T. S., et al., "Measurement of Through-the-Thickness Variations of Mechanical Properties in SA508 Gr.3 Pressure Vessel Steels Using Ball Indentation Test Technique," *International Journal of Pressure Vessels and Piping*, 74, 1997, pp. 231-238.
- [7] Haggag, F. M., "Nondestructive and Localized Measurements of Stress-Strain Curves and Fracture Toughness of Ferritic Steels at Various Temperatures Using Innovative Stress-Strain Microprobe™ Technology," Report No. DOE/ER/82115-2, 1999.
- [8] Haggag, Fahmy M., "In-Situ Nondestructive Measurements of Key Mechanical Properties of Oil and Gas Pipelines," *ASME PVP-Vol. 429*, 2001, pp. 99-104.
- [9] Byun, T. S., et al., "A Theoretical Model for Determination of Fracture Toughness of Reactor Pressure Vessel Steels in the Transition Region from Automated Ball Indentation Test," *Journal of Nuclear Materials*, 252, 1998, pp. 187-194.
- [10] Haggag, F. M., "Nondestructive Determination of Yield Strength and Stress-Strain Curves of In-Service Transmission Pipelines Using Innovative Stress-Strain Microprobe™ Technology," Report No. ATC/DOT/990901, 1999.
- [11] Haggag, F. M., "Effects of Irradiation Temperature on Embrittlement of Nuclear Pressure Vessel Steels," *ASTM STP 1175*, 1993, pp. 172-185.
- [12] ASTM Standard E1921-97, "Standard Test Method for Determination of Reference Temperature,  $T_0$ , for Ferritic Steels in the Transition Range," *Annual Book of ASTM Standards*, Vol 03.01.
- [13] Rolfe, Stanley T. and Barsom, John M., *Fracture and Fatigue Control in Structures: Applications of Fracture Mechanics*, Prentice-Hall, Inc., Englewood Cliffs, New Jersey, 1977, p. 129.